SUPPORTING INFORMATION

“Madelung Strain in Cuprate Superconductors – A Route to Enhancement of the Critical Temperature”

by V. Y. Butko, G. Logvenov, N. Bozovic, Z. Radovic and I. Bozovic[*]

In Figure S1, we show a photograph of the oxide molecular-beam epitaxy (MBE) system at BNL. A representative RHEED diffractogram obtained during growth of a La_2CuO_4 film is shown in Figure S2, the corresponding RHEED oscillation patterns in Figures S3 and S4. In Figure S5 we show a typical AFM image of the surface of such a film, showing rms surface roughness of no more than few Ångstroms. In Figure S6 we show the temperature dependence of resistivity data for single-phase I, M, and S films, and in Figure S7 the magnetic susceptibility data for I-M, M-I, and M-S bilayers, respectively, measured by the mutual inductance technique.

Figures 8-17 display X-ray data taken from various single-phase and bilayer films under study. The diffractograms demonstrate excellent epitaxial quality of the films. One can see from typical 2θ-ω scans for I, M, S, I-M, M-I, and M-S samples (Figures S8-S13, respectively) that all the (0, 0, L) diffraction peaks, with L = 2, 4, 6, 8, 10, 12 and 14, from the film and from the substrate are well resolved and that there are no peaks indicative of secondary-phase precipitates. The finite thickness fringes observed in Figures S14 and S15 are an indication of exceptional smoothness of the film surface. The angular distance between these fringes is consistent with the nominal thicknesses of the deposited film. The typical rocking curves (Figure S16) are very sharp, with FWHM of $0.03\text{-}0.06^0$, indicative of very little mosaicity in the films. A 3-dimensional image of X-ray diffraction intensity from a typical M-I sample measured in the 2-dimensional 2θ/ω - ω scan is presented in Figure S17. It shows that there is no peak of intensity in the reciprocal space region where one would expect to see a diffraction maximum from a bulk I layer (at 2θ ~ 110^0).

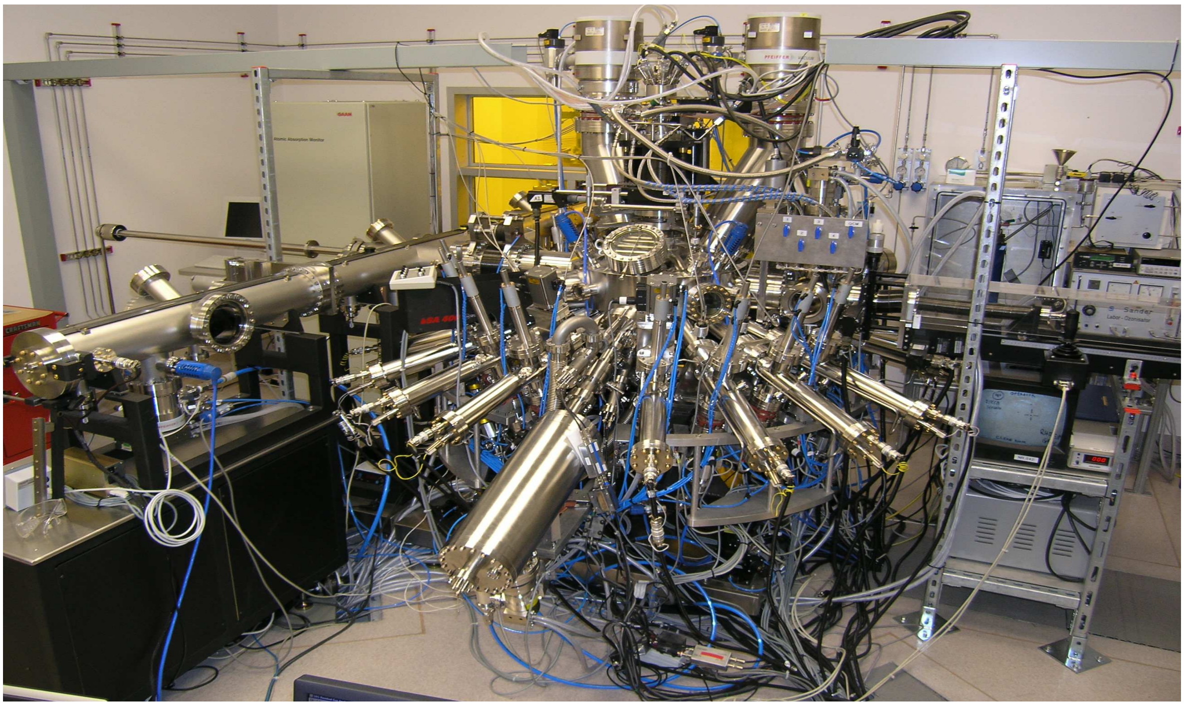

Figure S1. The atomic-layer-by-layer molecular beam epitaxy (ALL-MBE) system at Brookhaven National Laboratory. It enables synthesis of thin films and multilayers of cuprate superconductors with atomically smooth surfaces and interfaces, and allows for the digital control of the layer thickness.

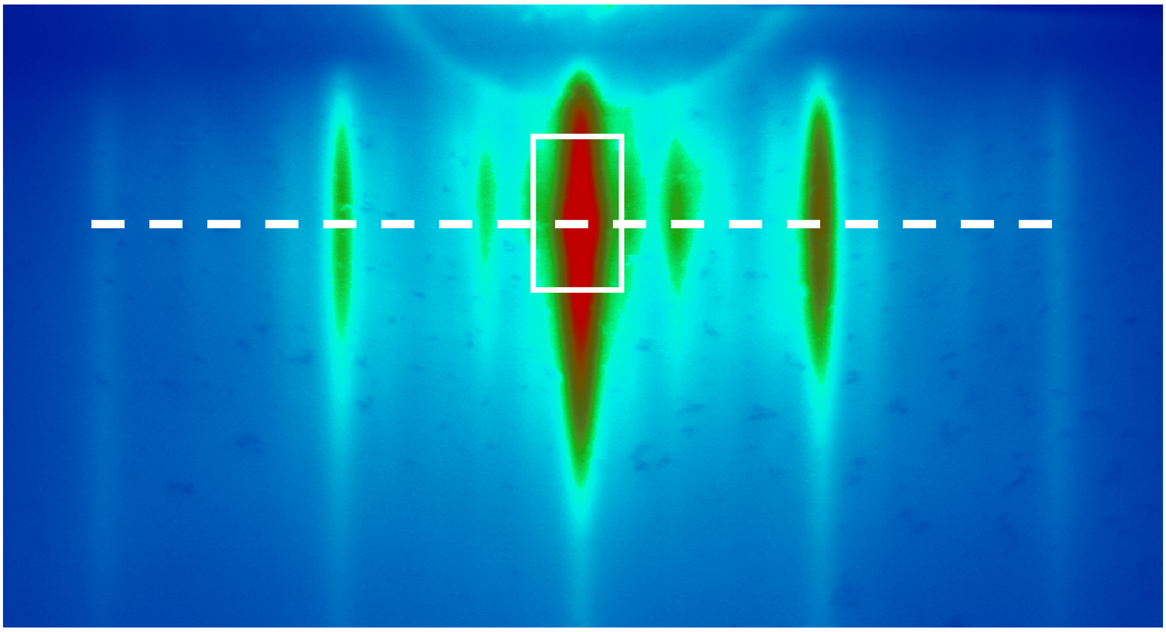

Figure S2. RHEED pattern during growth of La_2CuO_4 layer. The intensity is color-coded for better visibility. The electron beam is nearly parallel to the (100) direction. The spacing between the major streaks corresponds to the in-plane lattice spacing a_0 = 3.8 A. Four weaker side-bands are visible between each pair of main diffraction streaks, indicating some surface reconstruction with five time larger lattice spacing. The pattern changes periodically during deposition.

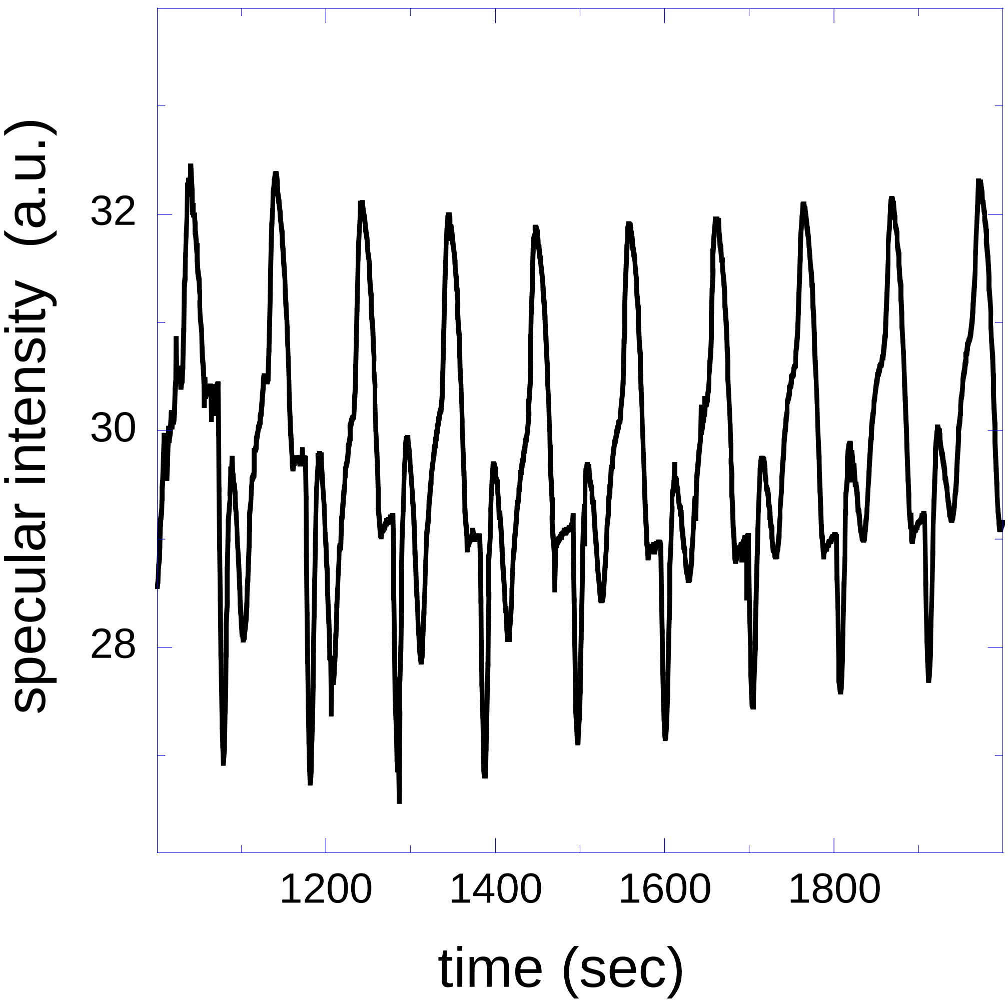

Figure S3. The time-dependence of the intensity of specular RHEED reflection (integrated over the area indicated by the white square in Figure S2), during growth of a La_2CuO_4 film.

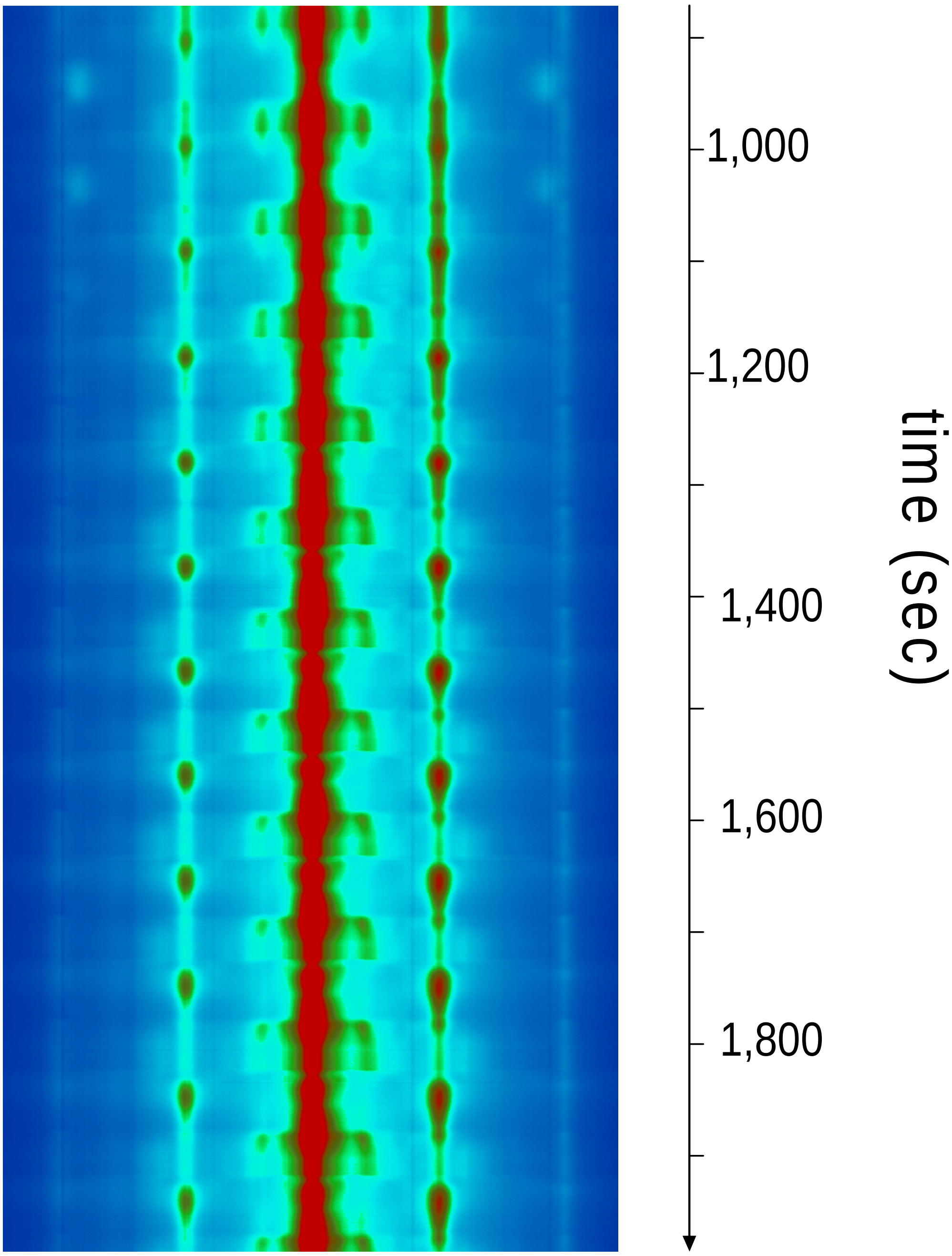

Figure S4. The time-dependence of RHEED intensity as a function of position along the dashed white line shown in Figure S2, during growth of a La_2CuO_4 film. The intensity is color-coded the same way as in Figure S2. The time-flow arrow is downwards.

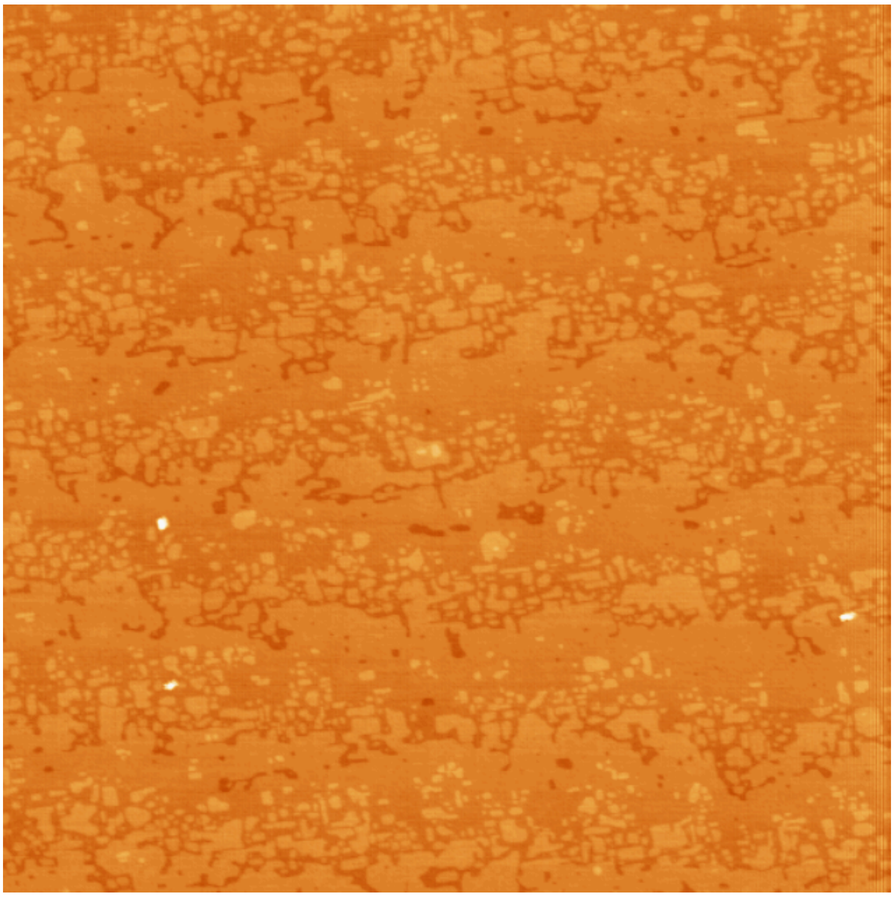

Figure S5. A typical Atomic Force Microscopy image of an M-I film on LSAO substrate. It shows rms surface roughness of 0.29 nm over a large area of 25 μm^2. Other films studied in the present work have shown similar surface quality.

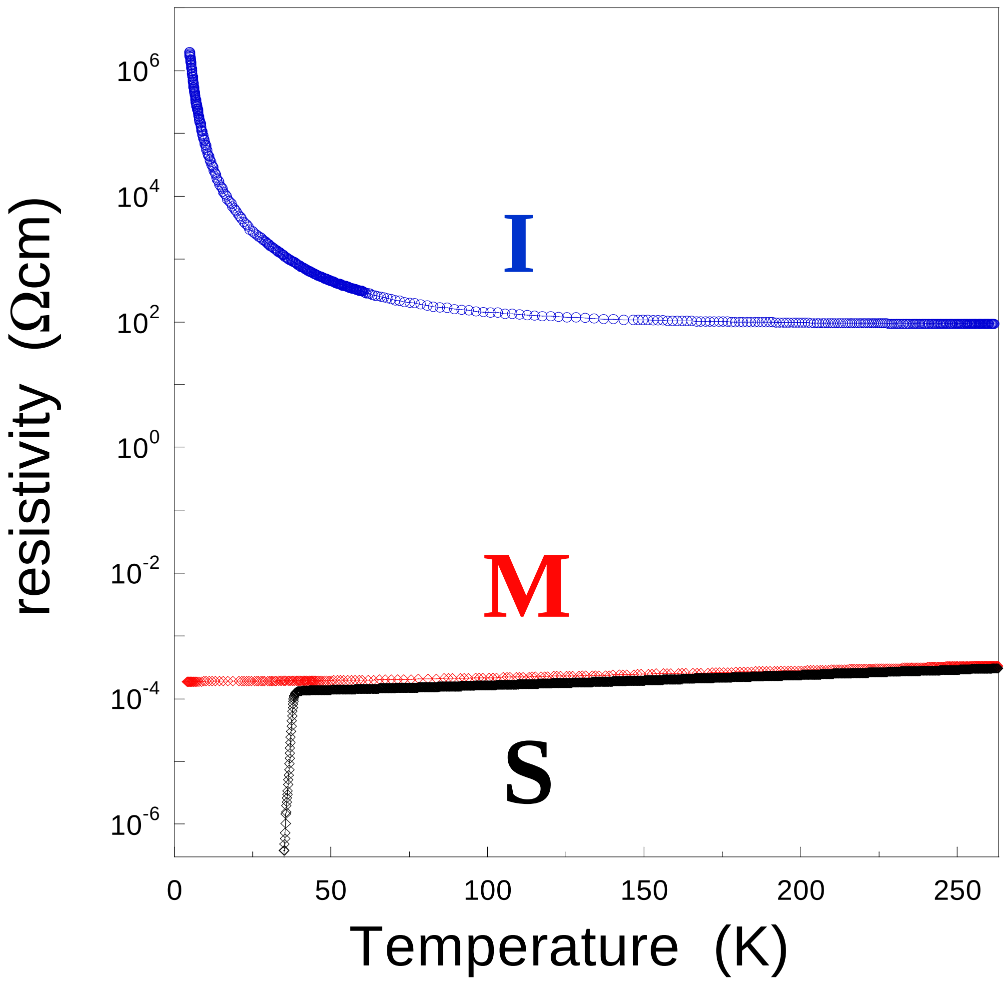

Figure S6. Resistivity vs. temperature data for typical I = La_2CuO_4, M = $La_{1.55}Sr_{0.45}CuO_4$, and S = $La_2CuO_{4+\delta}$ films.

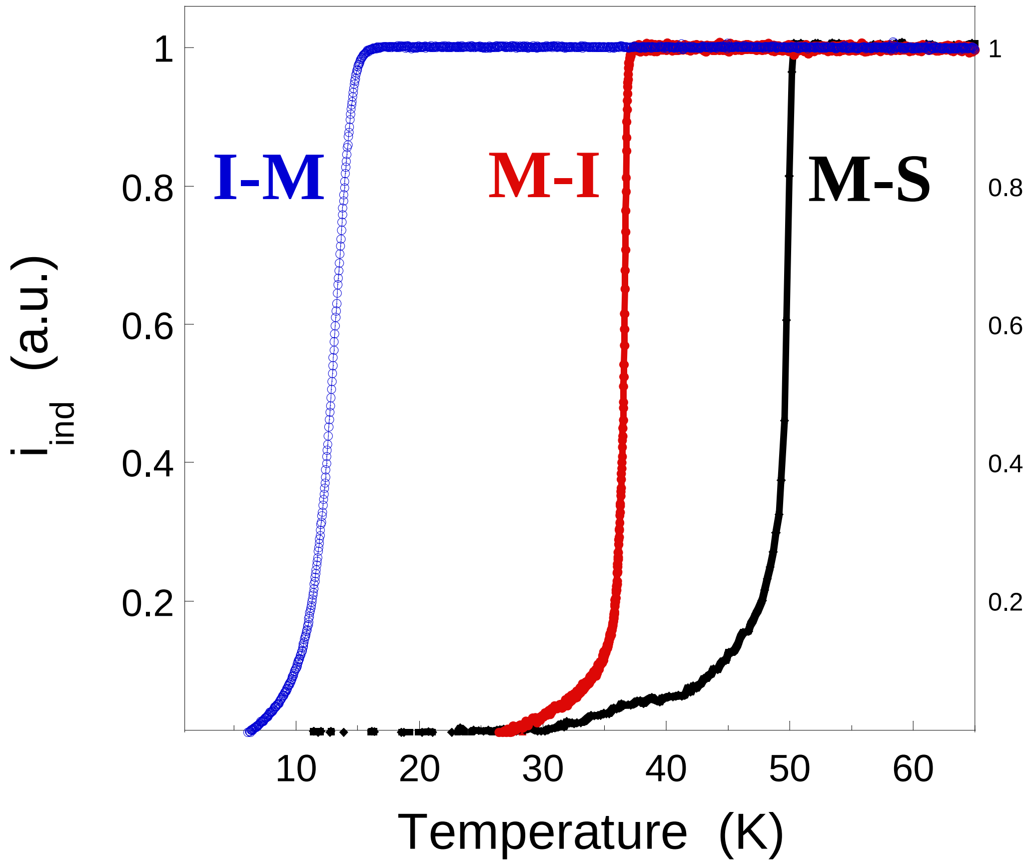

Figure S7. Mutual inductance vs. temperature data for typical I-M, M-I, and M-S bilayers, showing T_c ≈15 K, T_c ≈ 36 K and T_c ≈ 51 K, respectively. Here, i_{ind} is the out-of-phase (reactive) component of the current induced in the pick-up coil, placed on the opposite side of the film from the drive coil; it is determined by the drive coil current and the geometry (which are the same for all three samples), and the magnetic susceptibility of the film.

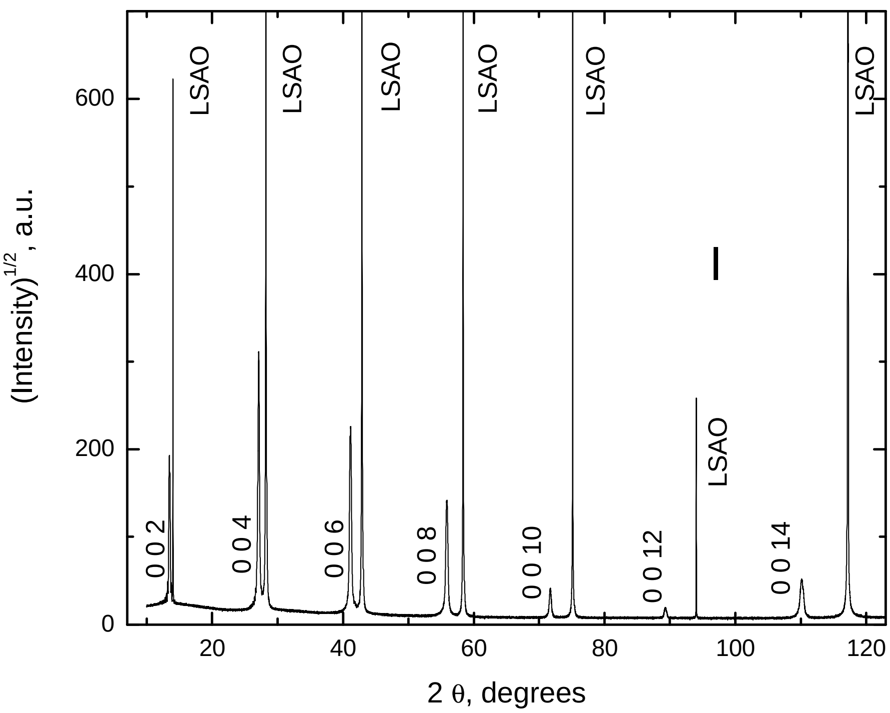

Figure S8. X-ray diffraction of an I film on LSAO substrate: 2Θ−ω scan taken over a large angle range. The film is 40 UC (52 nm) thick. The diffractogram shows sharp (0, 0, L) peaks with L = 2, 4, ..., 14, of both the film and the substrate. No other peaks, such as would originate from secondary phase precipitates, are detectable. The same is true of all other samples studied here (Figures S9-S15).

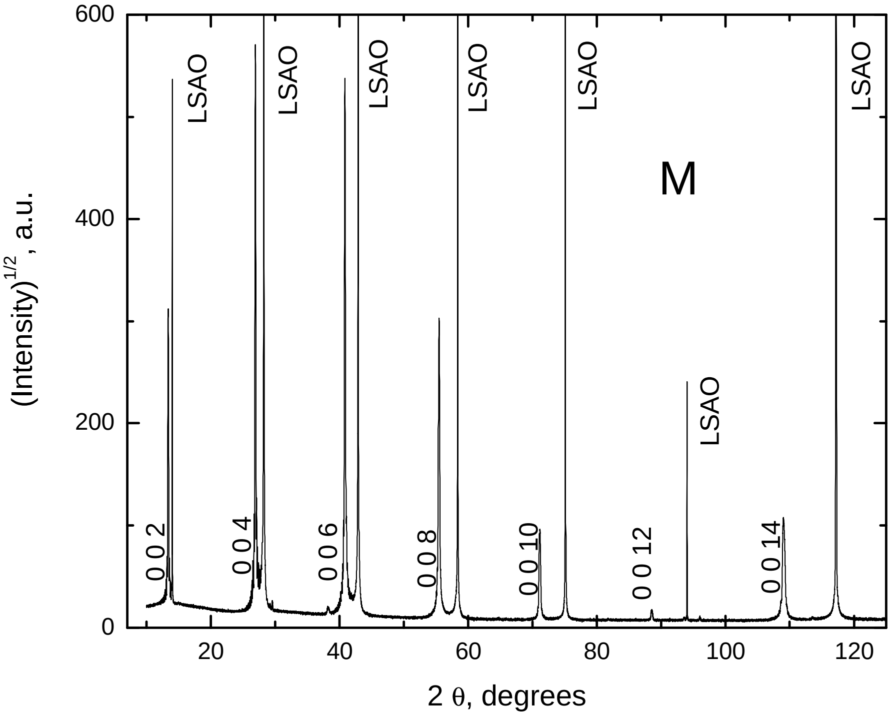

Figure S9. X-ray diffraction of an M film on LSAO substrate: 2Θ−ω scan taken over a large angle range. The film is 40 UC (52 nm) thick.

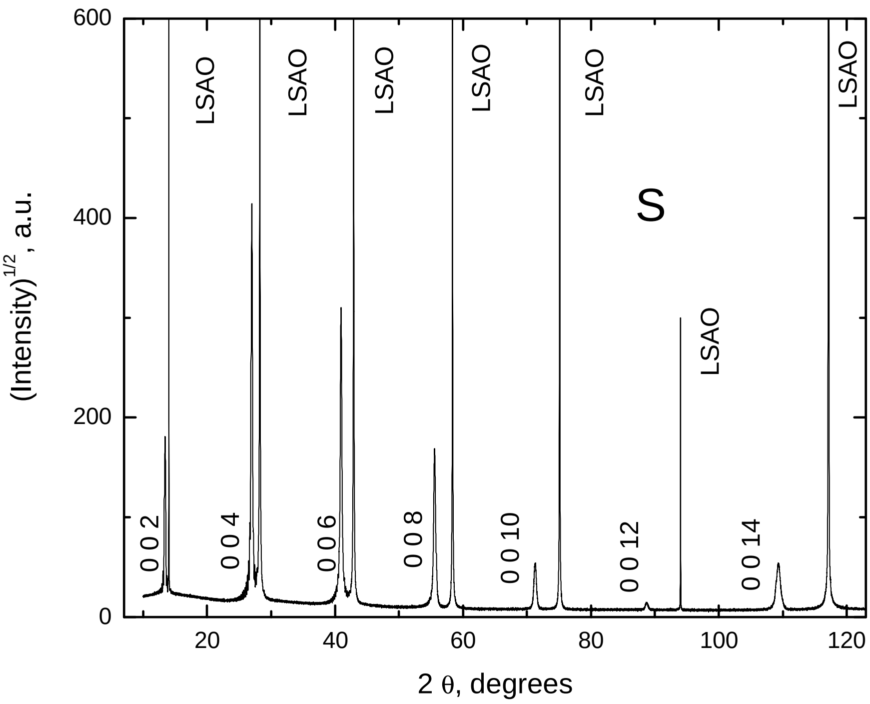

Figure S10. X-ray diffraction of an S film on LSAO substrate: $2\Theta-\omega$ scan taken over a large angle range. The film is 40 UC (52 nm) thick.

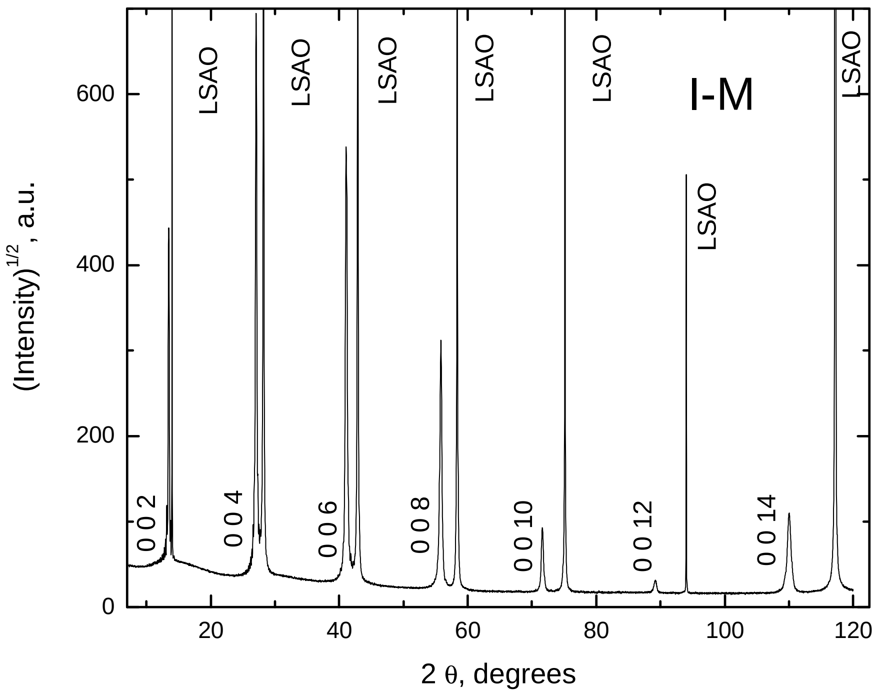

Figure S11. X-ray diffraction of an I-M bilayer film on LSAO substrate: 2Θ−ω scan taken over a large angle range. Each of the two layers is 20 UC (26 nm) thick.

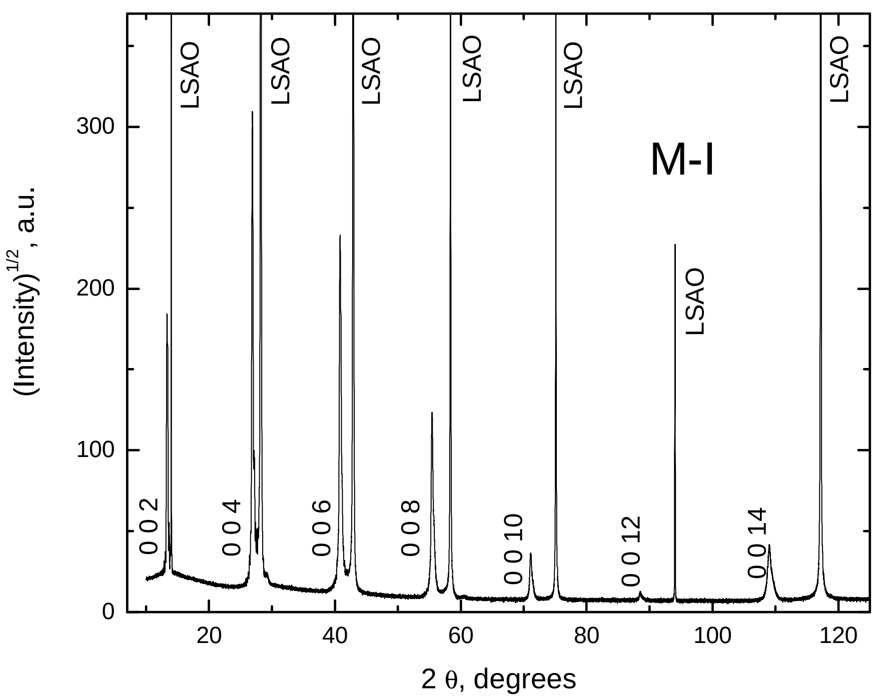

Figure S12. X-ray diffraction of an M-I bilayer film on LSAO substrate: 2Θ−ω scan taken over a large angle range. Each layer is 20 UC (26 nm) thick.

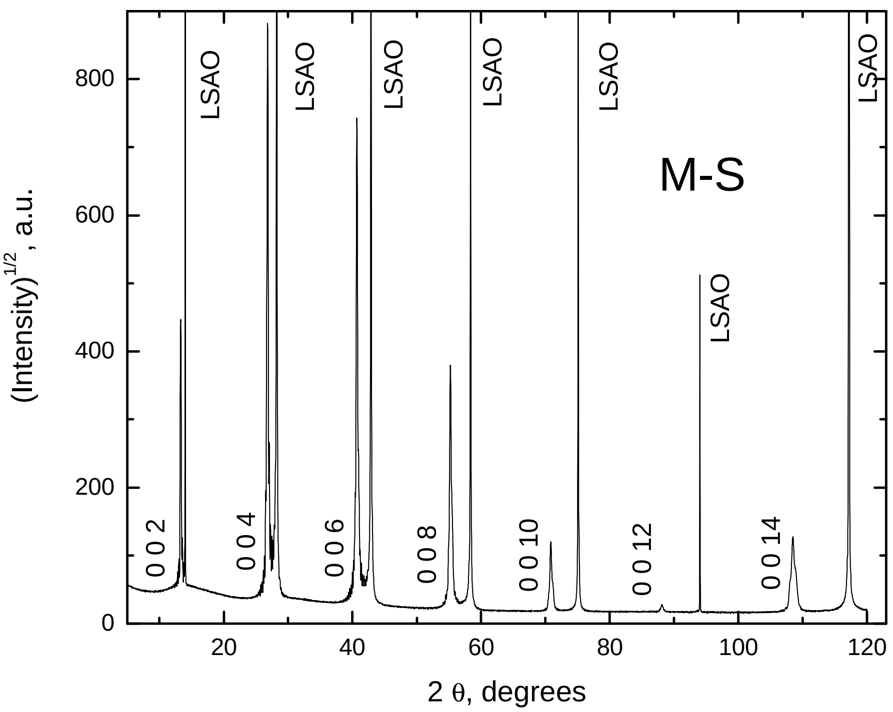

Figure S13. X-ray diffraction of an M-S bilayer film on LSAO substrate: 2Θ−ω scan taken over a large angle range. Each layer is 20 UC (26 nm) thick.

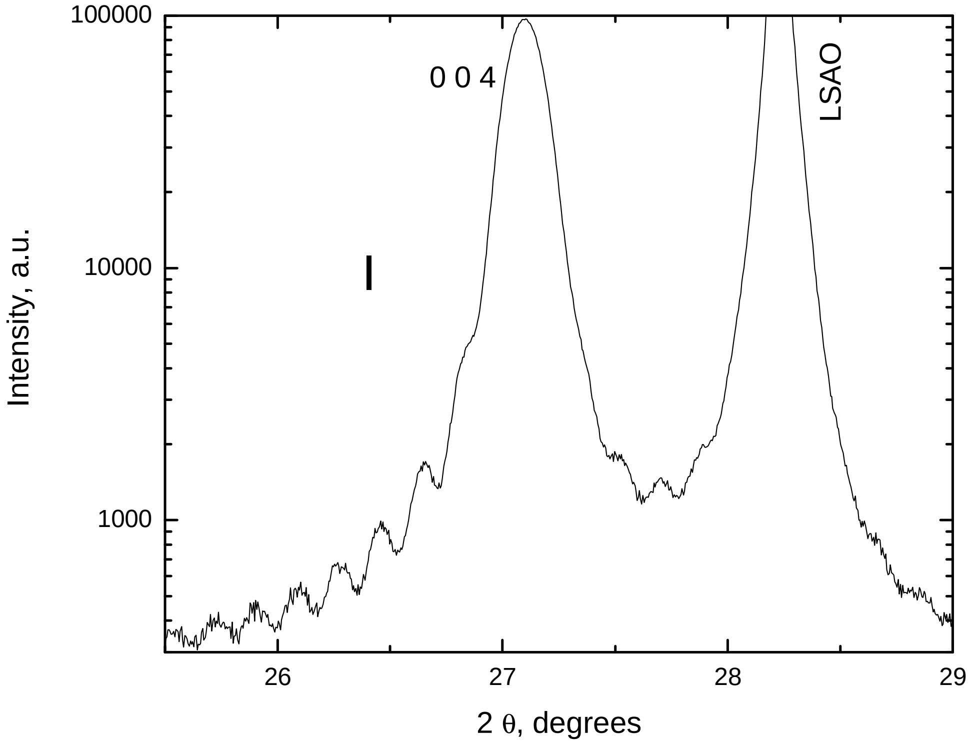

Figure S14. X-ray diffraction of an I film on LSAO substrate: 2Θ−ω scan taken near the (0,0,4) Bragg reflection. It shows pronounced finite-thickness oscillations, evidencing of the atomically smooth film surface and substrate/film interface.

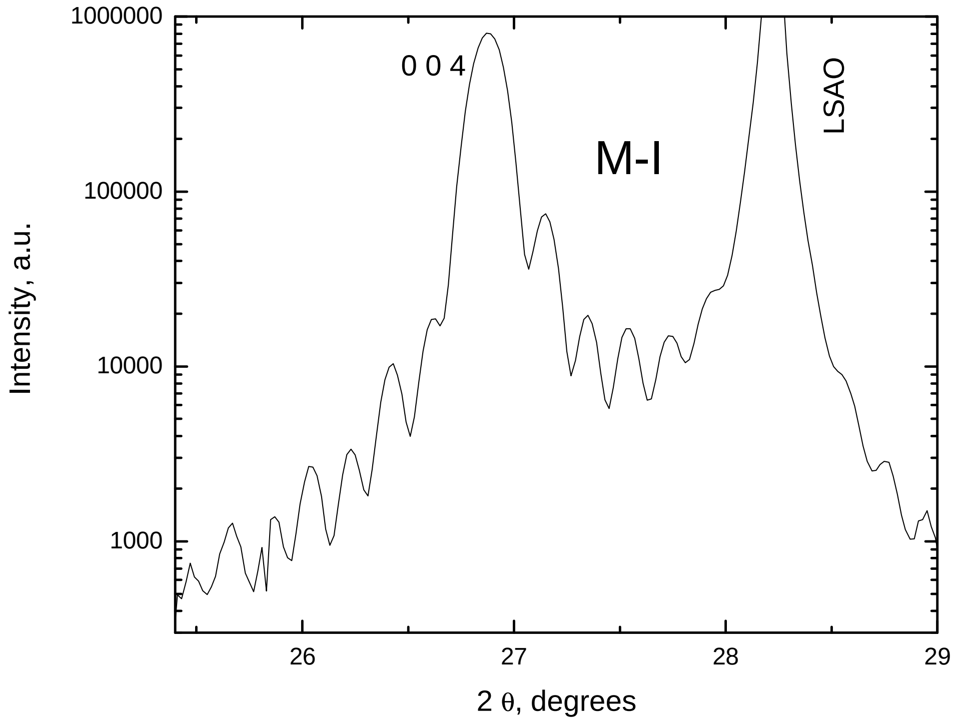

Figure S15. X-ray diffraction: 2Θ−ω scan taken near the (0,0,4) Bragg reflection of an M-I bilayer film on LSAO substrate. It shows pronounced finite-thickness oscillations, evidencing of the atomically smooth film surface and substrate/film interface.

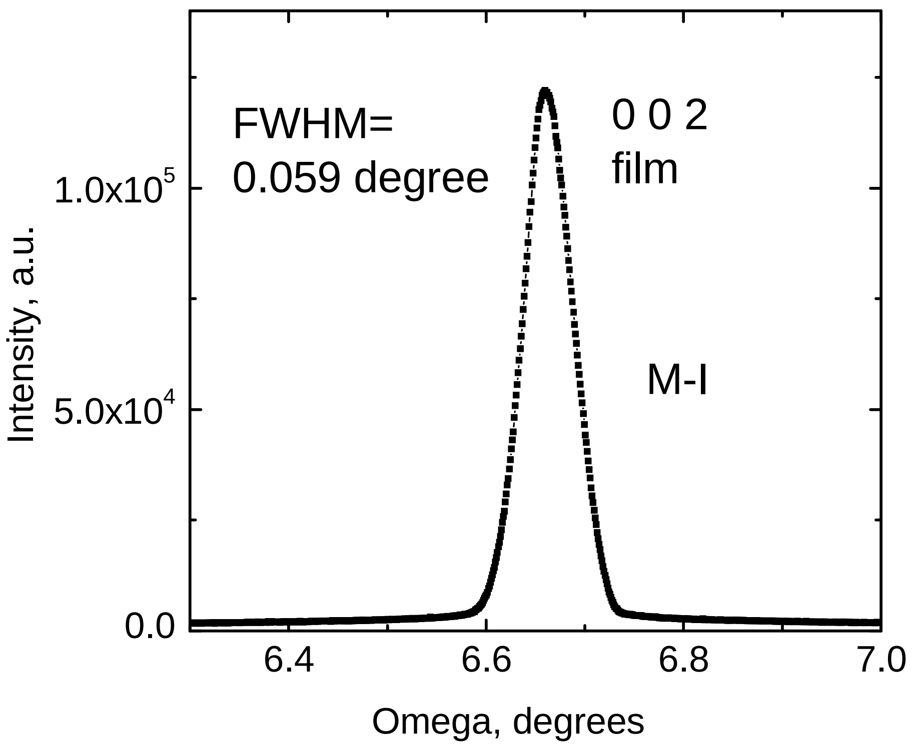

Figure S16. X-ray diffraction: the ω-rocking curve taken near the (0,0,2) Bragg reflection of an M-I bilayer film on LSAO substrate. The full width at the half maximum (FWHM) is very small, less then 0.06^0, which is comparable to that of the LSAO substrate itself. It indicates that there is very little mosaicity in the film.

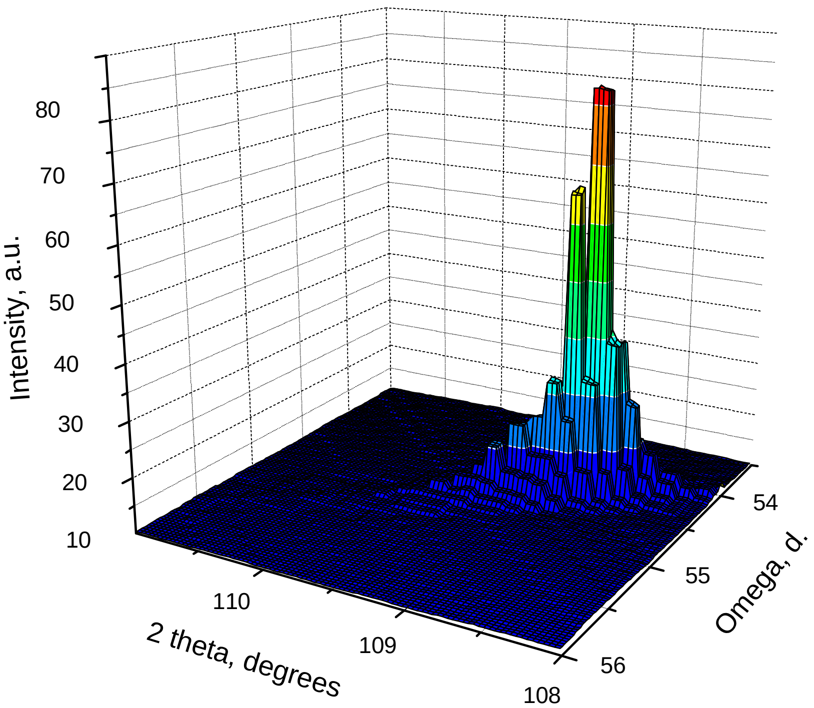

Figure S17. X-ray diffraction: the 2-dimensional scan, 2Θ–ω vs ω, taken near the (0,0,14) Bragg reflection of an M-I bilayer film on LSAO substrate. It shows that there is only a single peak; there is no large peak splitting (~1^0) such as would be expected if each of the two layers retained their nominal bulk structure. [See the simulated patterns in Figures 1c and 1d in the main text.]